
Comparison of ^{11}C -Pittsburgh Compound B and ^{18}F -Flutemetamol White Matter Binding in PET

Burcu Zeydan^{1,2}, Christopher G. Schwarz¹, Scott A. Przybelski³, Timothy G. Lesnick³, Walter K. Kremers³, Matthew L. Senjem^{1,4}, Orhun H. Kantarci², Paul H. Min¹, Bradley J. Kemp¹, Clifford R. Jack, Jr.¹, Kejal Kantarci¹, and Val J. Lowe¹

¹Department of Radiology, Mayo Clinic, Rochester, Minnesota; ²Department of Neurology, Mayo Clinic, Rochester, Minnesota;

³Department of Quantitative Health Sciences, Mayo Clinic, Rochester, Minnesota; and ⁴Department of Information Technology, Mayo Clinic, Rochester, Minnesota

PET imaging with β -amyloid ligands is emerging as a molecular imaging technique targeting white matter integrity and demyelination. β -amyloid PET ligands such as ^{11}C -Pittsburgh compound B (^{11}C -PiB) have been considered for quantitative measurement of myelin content changes in multiple sclerosis, but ^{11}C -PiB is not commercially available given its short half-life. A ^{18}F PET ligand such as flutemetamol with a longer half-life may be an alternative, but its ability to differentiate white matter hyperintensities (WMH) from normal-appearing white matter (NAWM) and its relationship with age remains to be investigated. **Methods:** Cognitively unimpaired (CU) older and younger adults ($n = 61$) were recruited from the community responding to a study advertisement for β -amyloid PET. Participants prospectively underwent MRI, ^{11}C -PiB, and ^{18}F -flutemetamol PET scans. MRI fluid-attenuated inversion recovery images were segmented into WMH and NAWM and registered to the T1-weighted MRI. ^{11}C -PiB and ^{18}F -flutemetamol PET images were also registered to the T1-weighted MRI. ^{11}C -PiB and ^{18}F -flutemetamol SUV ratios (SUVrs) from the WMH and NAWM were calculated using cerebellar crus uptake as a reference for both ^{11}C -PiB and ^{18}F -flutemetamol. **Results:** The median age was 38 y (range, 30–48 y) in younger adults and 67 y (range, 61–83 y) in older adults. WMH and NAWM SUVrs were higher with ^{18}F -flutemetamol than with ^{11}C -PiB in both older ($P < 0.001$) and younger ($P < 0.001$) CU adults. ^{11}C -PiB and ^{18}F -flutemetamol SUVrs were higher in older than in younger CU adults in both WMH ($P < 0.001$) and NAWM ($P < 0.001$). ^{11}C -PiB and ^{18}F -flutemetamol SUVrs were higher in NAWM than WMH in both older ($P < 0.001$) and younger ($P < 0.001$) CU adults. There was no apparent difference between ^{11}C -PiB and ^{18}F -flutemetamol SUVrs in differentiating WMH from NAWM in older and in younger adults. **Conclusion:** ^{11}C -PiB and ^{18}F -flutemetamol show a similar topographic pattern of uptake in white matter with a similar association with age in WMH and NAWM. ^{11}C -PiB and ^{18}F -flutemetamol can also effectively distinguish between WMH and NAWM. However, given its longer half-life, commercial availability, and higher binding potential, ^{18}F -flutemetamol can be an alternative to ^{11}C -PiB in molecular imaging studies specifically targeting multiple sclerosis to evaluate white matter integrity.

Key Words: PET; white matter hyperintensity; normal appearing white matter; ^{11}C -Pittsburgh compound B; ^{18}F -flutemetamol

J Nucl Med 2022; 63:1239–1244

DOI: 10.2967/jnumed.121.263281

PET imaging with β -amyloid ligands is largely used in the field of dementia clinically, but it is also emerging as a molecular imaging technique targeting various aspects in multiple sclerosis (MS) including demyelination (1–10), which correlate well with clinical disability (6) and cognition (7,9).

Although advanced MRI techniques such as diffusion tensor imaging are widely used in evaluating white matter (WM) integrity, they are not specific measures of myelin. Over the last decade, PET ligands have been used to study myelin kinetics (1–11). PET ligands are also being used to understand the underlying mechanisms such as neuroinflammation, neurodegeneration, microglia activation, and myelin kinetics (11,12). PET ligands have also been proposed as a potential outcome measure in clinical trials (11), which would be especially important for future remyelination trials potentially adding value to MRI alone. Among these ligands, ^{11}C -Pittsburgh compound B (^{11}C -PiB) seems to be a sensitive and reliable imaging marker in measuring WM integrity and potentially myelin integrity both in animal and in human studies (2,3,5–8).

^{11}C -PiB uptake in the WM correlates with well-established WM integrity imaging markers such as diffusion tensor imaging (8) as well as cognitive function (7–9). Consistent with that, WM ^{11}C -PiB uptake is lower in white matter hyperintensities (WMH). On the other hand, white matter ^{11}C -PiB uptake increases with aging (8,13). This seems rather contradictory as WMH volume also increases with aging, and ^{11}C -PiB uptake is lower in WMH than normal-appearing white matter (NAWM), with uptake in both compartments increasing with aging suggesting that the aging and WMH effects are independently influencing ^{11}C -PiB uptake in the WM. ^{11}C -PiB shows high affinity for WM; however, given its short half-life (20 min), it is not commercially available. To conduct multicenter clinical trials using PET imaging to investigate WM integrity and to make PET imaging more accessible, ^{18}F PET ligands such as ^{18}F -flutemetamol may be a more reliable alternative.

Furthermore, PET ligand uptake in the WM is increasingly being used as a reference region to calculate the SUV ratios (SUVrs) in longitudinal β -amyloid PET studies (14–18). Thus, the association between WM ^{11}C -PiB uptake and aging should be carefully considered in serial β -amyloid PET studies and should be investigated further with different PET ligands such as flutemetamol to see if there is a similar variation of WM ^{18}F -flutemetamol uptake.

Both ^{11}C -PiB and ^{18}F -flutemetamol PET ligands have been investigated as potential WM integrity markers in animal and human studies on PET imaging (11). Although PET ligands are not identical in their uptake characteristics, their topographic patterns of uptake may

Received Sep. 28, 2021; revision accepted Nov. 30, 2021.

For correspondence or reprints, contact Val J. Lowe (vlowe@mayo.edu).

Published online Dec. 16, 2021.

COPYRIGHT © 2022 by the Society of Nuclear Medicine and Molecular Imaging.

be comparable. In the current study, WM was evaluated in 2 compartments, WMH and NAWM, in cognitively unimpaired (CU) younger and older adults, and the ability of ^{11}C -PiB and ^{18}F -flutemetamol PET ligands to differentiate WMH from NAWM was investigated.

MATERIALS AND METHODS

Study Population

CU older adults with an age range of 61–83 y and younger adults with an age range of 30–48 y were recruited from the community responding to a study advertisement for β -amyloid PET (13). Although it is expected to be more significant in older adults, WMH increases with aging across the adult life span including younger adults. Moreover, WMH is clinically relevant in terms of its association with higher blood pressure and higher HbA1C even in younger adults with low WMH (19).

To compare WM binding characteristics of 2 ligands (^{11}C -PiB and ^{18}F -flutemetamol), the participants prospectively underwent MRI, ^{11}C -PiB, and ^{18}F -flutemetamol PET scanning. The ^{11}C -PiB and ^{18}F -flutemetamol scans were completed within a median of 4 d. No adverse events were seen from imaging.

Imaging Acquisitions and Analyses

PET imaging was performed using a PET/CT scanner (DRX or DRXT; GE Healthcare) operating in 3-dimensional (3D) mode using ^{11}C -PiB and ^{18}F -flutemetamol tracers. ^{11}C -PiB PET images were acquired in 20 min (in four 5-min dynamic frames), after an injection of ^{11}C -PiB (555 MBq; range, 292–729 MBq) with a 40-min uptake delay. ^{18}F -flutemetamol PET images were also acquired in 20 min, after an injection of ^{18}F -flutemetamol (370 MBq; range, 333–407 MBq) with an 80-min uptake delay (20). To create a single static PET image, dynamic frame images were averaged. An iterative reconstruction algorithm was applied with a 5-mm gaussian postprocessing filter, and attenuation, scatter, and random coincidences as well as radioactive decay were corrected (18).

An automated imaging processing pipeline was used to analyze PET images (18). The cerebellar crus gray matter was used as a reference region to create normalized ^{11}C -PiB and ^{18}F -flutemetamol PET SUVr images, which is a previously established reference region in PET studies that target WM in both CU individuals and patients with MS (7,8). For anatomic segmentation and labeling of WMH and NAWM, MRI was performed on 3.0-T scanners (GE Healthcare), which included a T2-weighted fluid-attenuated inversion recovery (FLAIR) sequence and a T1-weighted 3D high-resolution magnetization-prepared rapid acquisition gradient-echo (MPRAGE) sequence (21). First, a semiautomated segmentation algorithm on FLAIR-MRI was used to segment WM into WMH and NAWM (22). Then, FLAIR images were coregistered to MPRAGE images and MPRAGE images were segmented using SPM12 with the Mayo Clinic Adult Life span Template (<https://www.nitrc.org/projects/mcalt/>) (23). A WM mask was generated using a threshold for SPM12 WM segmentation to include voxels with probability ≥ 0.5 . To account for T1-hypointense lesions being erroneously called gray matter, voxels segmented as WMH in the coregistered FLAIR images were also included as WM. To exclude voxels severely affected by partial-volume averaging of gray matter and cerebrospinal fluid, the WM mask was eroded by 3 mm. The remaining WM voxels were divided into 2 subclass masks, WMH and NAWM. Finally, the mean value for each of ^{11}C -PiB and ^{18}F -flutemetamol PET SUVrs over all voxels in each of the WMH and NAWM segmentation masks was calculated.

Study Consent

The study protocol was approved by the Mayo Clinic institutional review board. Informed consent was obtained from each participant.

Statistical Analysis

Participants' characteristics were compared among younger and older CU adults using t tests for continuous variables or χ^2 tests for categorical variables. Due to the gap in ages from 48 to 61, all analyses were stratified by younger and older adult age groups. Amyloid imaging SUVrs were compared using paired t tests for pairwise group comparisons. Linear regression models and Pearson correlations were used for testing the association of age with ^{11}C -PiB and ^{18}F -flutemetamol SUVrs in WMH and NAWM. To compare associations of ^{11}C -PiB SUVr with ^{18}F -flutemetamol between WMH and NAWM, we used linear mixed models adjusted for age, across all participants, with 2 values (WMH and NAWM) per participant. The mixed models accounted for within-participant correlations. We used a group variable for WMH/NAWM and tested for an interaction by group. A significant interaction would indicate a difference in slopes for WMH and NAWM. To compare the performance of ^{11}C -PiB and ^{18}F -flutemetamol tracers in groupwise regional differentiation (WMH vs. NAWM), the area under the receiver-operating-characteristic curve (AUROC) generated using a simultaneous 2-stage parameter estimation approach (24) was used. Each AUROC had 95% CIs estimated using the bootstrap method. All tests used an α level of 0.05 for significance.

RESULTS

CU older adults ($n = 31$) had a median age of 67 y (range, 61–83 y), and CU younger adults ($n = 30$) had a median age of 38 y (range, 30–48 y). Sex, *APOE* $\epsilon 4$ carrier status, and years of education were not different between the groups. As expected, the WMH volume was higher ($P < 0.001$) in older CU ($16.74 \pm 27.01 \text{ cm}^3$) than younger CU adults ($2.90 \pm 1.65 \text{ cm}^3$) (Table 1).

^{11}C -PiB SUVr Compared with ^{18}F -Flutemetamol SUVr in WMH and NAWM

WMH SUVrs were higher with ^{18}F -flutemetamol than with ^{11}C -PiB in both younger ($P < 0.001$) and older CU ($P < 0.001$) adults. Similarly, NAWM SUVrs were higher with ^{18}F -flutemetamol than with ^{11}C -PiB in both younger ($P < 0.001$) and older CU ($P < 0.001$) adults.

WM ^{11}C -PiB and ^{18}F -Flutemetamol SUVr in Younger Compared with Older CU Adults

^{11}C -PiB SUVr was lower in WMH ($P < 0.001$) in younger than in older CU adults. ^{11}C -PiB SUVr was also lower in NAWM ($P < 0.001$) in younger than in older CU adults. Similarly, ^{18}F -flutemetamol SUVr was lower in the WMH ($P < 0.001$) and NAWM ($P < 0.001$) in younger than in older CU adults (Table 1; Fig. 1). In addition, age correlated with higher WMH ^{11}C -PiB SUVr in younger CU adults ($r = 0.43$; $P = 0.018$) and with higher NAWM ^{11}C -PiB SUVr in older CU adults ($r = 0.38$; $P = 0.037$) (Fig. 2). The slopes of the association between age and ^{11}C -PiB compared with age and ^{18}F -flutemetamol in WMH was not different in older CU adults ($P = 0.16$). The slopes of the association between age and ^{11}C -PiB compared with age and ^{18}F -flutemetamol in WMH was not different in younger CU adults ($P = 0.41$). Similarly, the slopes of association between age and ^{11}C -PiB compared with age and ^{18}F -flutemetamol in NAWM was not different in older CU adults ($P = 0.26$). The slopes of association between age and ^{11}C -PiB compared with age and ^{18}F -flutemetamol in NAWM was not different in younger CU adults ($P = 0.16$) (Fig. 2).

^{11}C -PiB and ^{18}F -Flutemetamol SUVr in WMH Compared with ^{11}C -PiB and ^{18}F -Flutemetamol SUVr in NAWM

^{11}C -PiB SUVr in WMH was lower than in NAWM in both younger and older CU adults ($P < 0.001$). Similarly, ^{18}F -flutemetamol

TABLE 1
Participants' Demographic and Imaging Characteristics

Demographic	All (n = 61)	Younger CU (n = 30)	Older CU (n = 31)	P
Age (y)	53.7 (15.8)	38.9 (6.0)	68.1 (5.8)	<0.001
Males (n)	23 (38%)	12 (40%)	11 (35%)	0.72
APOE ε4 (n)*	17 (29%)	11 (38%)	6 (21%)	0.15
Education (y)	15.1 (2.0)	15.5 (2.0)	14.7 (2.0)	0.17
WMH volume (cm ³)	9.94 (20.36)	2.90 (1.65)	16.74 (27.01)	<0.001
PiB SUVr WM	1.92 (0.20)	1.81 (0.13)	2.02 (0.20)	<0.001
PiB SUVr WMH	1.75 (0.19)	1.65 (0.13)	1.85 (0.20)	<0.001
PiB SUVr NAWM	1.92 (0.21)	1.81 (0.13)	2.04 (0.20)	<0.001
FMT SUVr WM	2.42 (0.25)	2.29 (0.14)	2.53 (0.28)	<0.001
FMT SUVr WMH	2.14 (0.25)	2.03 (0.15)	2.25 (0.28)	<0.001
FMT SUVr NAWM	2.43 (0.25)	2.29 (0.14)	2.56 (0.27)	<0.001

*3 are missing APOE ε4

Mean with SD in parentheses listed for continuous variables and count with % in parentheses for the categorical variables. P values comparing groups are from a t test or χ-squared test.

FMT = ¹⁸F-flutemetamol.

SUVr in WMH was lower than in NAWM ($P < 0.001$) in both younger and older CU adults (Fig. 1). In younger CU adults, the AUROC comparing WMH versus NAWM for ¹¹C-PiB was 0.828 (95% CI, 0.747–0.903) and for ¹⁸F-flutemetamol it was 0.902 (95% CI, 0.821–0.982). In older CU adults, the AUROC comparing WMH versus NAWM for ¹¹C-PiB was 0.751 (95% CI, 0.692–0.794) and for ¹⁸F-flutemetamol it was 0.787 (95% CI, 0.725–0.845). AUROC analysis suggested no difference between ¹¹C-PiB and ¹⁸F-flutemetamol SUVr in differentiating WMH from NAWM in both younger and older adults.

DISCUSSION

β-amyloid PET ligands were originally developed for measuring cortical β-amyloid deposition in Alzheimer disease. However, independent of the presence of cortical β-amyloid deposition,

WM uptake is also observed in β-amyloid PET studies (25,26). Recently, β-amyloid PET ligands have been specifically repurposed as potential markers of WM integrity in MS due to an ongoing need for molecular imaging ligands for myelin in MS. None of the existing advanced imaging techniques target myelin specifically. By contrast, β-amyloid PET ligands have showed high affinity to WM with high sensitivity and sensitivity to myelin (1,27). Therefore, β-amyloid PET ligands can successfully differentiate WMH from NAWM (7,8). Moreover, β-amyloid PET ligand uptake decreases in demyelinating lesions and increases in ensuing remyelinated lesions (2,6,28), which generates the possibility of using molecular imaging as a biomarker for potential remyelination therapies. Changes in β-amyloid PET ligand uptake also correlate well with clinical disability scales (6) and cognitive performance (7,9) in patients with MS. Therefore, β-amyloid PET ligand uptake can be a perfect complementary metric to MRI in clinical trials targeting myelin integrity in MS.

Among the β-amyloid PET ligands, ¹¹C-PiB has emerged as a sensitive and reliable imaging marker in measuring WM integrity both in animal and in human studies (2,3,5–8). However, it also has a suboptimal signal-to-noise ratio and a short half-life ($T_{1/2} = 20$ min), making it challenging to be widely used and commercially available. ¹⁸F-flutemetamol, which is a fluorinated analog of ¹¹C-PiB, has been developed to increase the availability of β-amyloid PET by compensating for the short half-life of ¹¹C-PiB ligand (20).

In the current study, we compared ¹¹C-PiB and ¹⁸F-flutemetamol PET ligands in WMH and NAWM in different age groups. We found that WMH and NAWM SUVrs were higher with ¹⁸F-flutemetamol than with ¹¹C-PiB in both older and younger CU adults. ¹¹C-PiB and ¹⁸F-flutemetamol uptake was higher in older than in younger CU

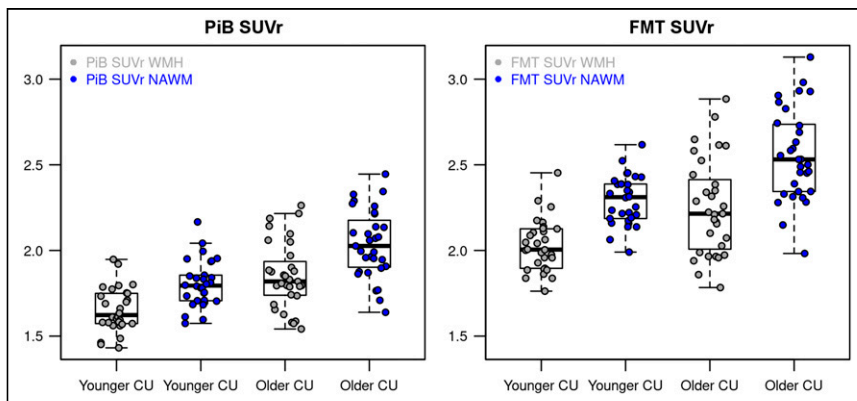


FIGURE 1. ¹¹C-PiB and ¹⁸F-flutemetamol SUVr in WMH and NAWM in younger and older CU adults. ¹¹C-PiB SUVr in WMH and NAWM was lower in younger than in older CU adults. ¹¹C-PiB SUVr in WMH was lower than in NAWM in both younger and older CU adults. ¹⁸F-flutemetamol SUVr in WMH and NAWM was lower in younger than in older CU adults. ¹⁸F-flutemetamol SUVr in WMH was lower than in NAWM in both younger and older CU adults. FMT = ¹⁸F-flutemetamol.

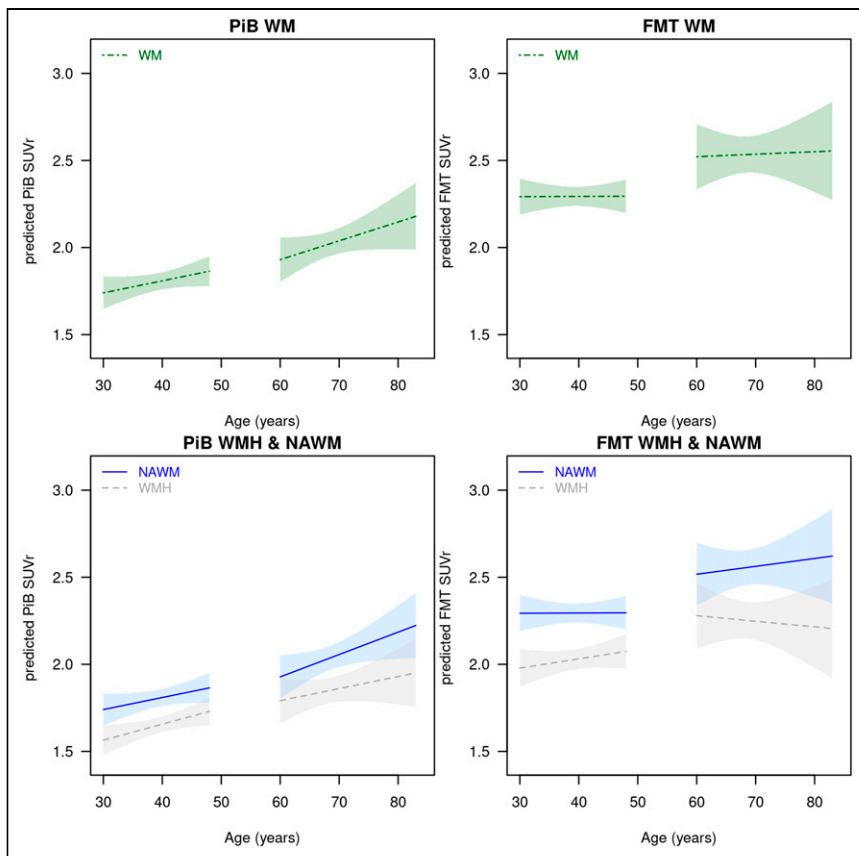


FIGURE 2. Association between age and ^{11}C -PiB and ^{18}F -flutemetamol in WM. (Top) Associations of ^{11}C -PiB and ^{18}F -flutemetamol radioligand uptake with age were compared in WM. (Bottom) Associations of ^{11}C -PiB and ^{18}F -flutemetamol radioligand uptake with age were compared in WMH and NAWM compartments individually. Slopes of association between age and ^{11}C -PiB compared with age and ^{18}F -flutemetamol in WMH were not different in older CU adults. Slopes of association between age and ^{11}C -PiB compared with age and ^{18}F -flutemetamol in WMH were not different in younger CU adults. Slopes of association between age and ^{11}C -PiB compared with age and ^{18}F -flutemetamol in NAWM were not different in older CU adults. Slopes of association between age and ^{11}C -PiB compared with age and ^{18}F -flutemetamol in NAWM were not different in younger CU adults. FMT = ^{18}F -flutemetamol.

adults in both WMH and NAWM. ^{11}C -PiB and ^{18}F -flutemetamol showed a similar topographic pattern of uptake in the WM, with higher uptake in NAWM than WMH in both older and younger CU adults. There was no difference between ^{11}C -PiB and ^{18}F -flutemetamol SUVrs in differentiating WMH from NAWM in both younger and older adults.

^{11}C -PiB and ^{18}F -flutemetamol have a similar diagnostic performance for detecting cortical β -amyloid deposition in CU adults and patients with AD (29,30). Although, compared with ^{11}C -PiB, a higher ^{18}F -flutemetamol uptake is commonly observed in the WM both visually (29,30) and quantitatively (13,31). However, less is known about the WMH and NAWM uptake differences between ^{11}C -PiB and ^{18}F -flutemetamol. In the current study, ^{18}F -flutemetamol SUVrs in the WMH and NAWM were higher than ^{11}C -PiB in both older and younger CU adults. Nevertheless, ^{11}C -PiB and ^{18}F -flutemetamol ligands were not superior to one another in differentiating WMH from NAWM in either age group. Similarly, a recent animal study showed a head-to-head comparison of WM binding using ^{11}C (^{11}C -PiB and ^{11}C -MEDAS) and ^{18}F (^{18}F -flutemetamol, ^{18}F -florbetaben, ^{18}F -florbetapir) PET ligands in 4 healthy nonhuman primates (baboons) (31) to study their ability to distinguish WM from gray matter binding. Consistent with our findings, ^{18}F PET ligands showed higher SUVrs

and higher binding potentials than ^{11}C PET ligands in the WM. It is speculated that several mechanisms may partially contribute to the variability in the amount of WM uptake between different PET ligands such as differences in molar activities, brain penetrance through the blood-brain barrier, and duration to reach a WM-gray matter equilibrium (31).

Both ^{11}C -PiB and ^{18}F -flutemetamol ligands showed a similar topographic pattern of uptake in the WM, with higher uptake in NAWM than in WMH. This is in line with previous findings in which ^{11}C -PiB PET imaging was used as a plausible WM integrity marker (1,3,4,6,7,28). Both animal and human studies show that ^{11}C -PiB PET may differentiate between myelinated tracts, demyelinated lesions (2,7), and remyelinated regions (3,6). A recent study demonstrated that lower ^{18}F -florbetapir uptake in WM correlated with large-caliber axon degeneration in Alzheimer disease spectrum, reinforcing previous findings on β -amyloid PET ligand uptake in the WM being myelin-dependent (32). The mechanism of β -amyloid tracers' uptake in the WM is not very well understood. However, the β -pleated structure of both the β -amyloid peptide and the myelin basic protein seems to be the common target of β -amyloid PET ligands (33,34). Moreover, the β -amyloid PET ligands are lipophilic in nature and this potentially contributes to the higher binding in the WM, which is also high in lipid content (35). The mechanism of PET ligand uptake in the WM may partly be also attributed to specific WM kinetics, mainly slower rates of regional clearance of the ligands in the WM (36). Alternatively, a dynamic PET acquisition method could be used to compare and explore

further WM binding patterns of ^{11}C -PiB and ^{18}F -flutemetamol (5). Furthermore, to better understand the differences in topographic uptake patterns of ^{11}C -PiB and ^{18}F -flutemetamol WM, a future study including patients with MS would be of interest.

^{11}C -PiB and ^{18}F -flutemetamol ligands also showed a similar pattern of uptake in both WMH and NAWM in association with age. There was higher ^{11}C -PiB and ^{18}F -flutemetamol uptake in older than in younger CU adults in both WMH and in NAWM. The comparison of slopes of association between age and PiB compared with age and ^{18}F -flutemetamol in WMH was not different in older or younger CU adults. Similarly, the comparison of slopes of association between age and ^{11}C -PiB compared with age and ^{18}F -flutemetamol in NAWM was also not different in older or younger CU adults. WM uptake significantly increases with aging (13,37). In parallel, WMH and NAWM uptake increase with aging as well (8,13). This may be in part due to reduced kinetics (36,38,39) and reduced global blood perfusion rate (40) in the WM with aging. The increase in PET ligand uptake in the WM with aging is an important factor to consider, because WM is increasingly used as a reference region in longitudinal PET imaging studies. Aging is associated with an increase of WMH volume along with a decrease in myelin integrity, which is expected to result in an overall decrease in PET ligand

uptake in the WM. However, in the current study, higher WMH and NAWM ^{11}C -PiB and ^{18}F -flutemetamol uptake was observed in the older compared with younger adults, in line with previous studies (8,37). This suggests that additional aging-related mechanisms may be influencing WM PET ligand uptake (8,37). Moreover, although ^{11}C -PiB and ^{18}F -flutemetamol show a similar topographic WMH and NAWM uptake in different age groups, there is also a quantitative difference between ^{11}C -PiB and ^{18}F -flutemetamol as ^{18}F -flutemetamol shows a higher uptake in WMH as well as in NAWM compared with ^{11}C -PiB. Therefore, when WM uptake is used as a reference region for the evaluation of cortical uptake in serial PET studies, age, WMH volume and the type of the PET tracer should be carefully considered in these calculations (8).

CONCLUSION

^{11}C -PiB can effectively distinguish between WMH and NAWM, but its lower overall binding capacity to WM and to the compartments of WMH and NAWM compared with ^{18}F -flutemetamol may result in a suboptimal signal-to-noise ratio (31). However, a lower signal-to-noise ratio seems to have no impact on the differentiation of WMH and NAWM with ^{11}C -PiB compared with ^{18}F -flutemetamol. With higher binding potentials along with longer half-lives, ^{18}F PET ligands such as ^{18}F -flutemetamol are alternatively positioned to be used in multicenter clinical trials targeting myelin repair as a secondary outcome in demyelinating diseases including MS. Such an outcome measure can potentially provide more myelin-specific information than MR diffusion tensor imaging metrics alone both as a complementary and as a stand-alone metric.

DISCLOSURE

Financial support for this study was provided by GE Healthcare Inc., NIH P50 AG16574, U01 AG06786, R37 AG11378, RO1 AG041851, U54 AG044170, and the Dekelbom Foundation. No other potential conflict of interest relevant to this article was reported.

KEY POINTS

QUESTION: Do ^{18}F -flutemetamol and ^{11}C -PiB show a similar topographic pattern of uptake in the WMH and NAWM as there is an ongoing need in MS for molecular imaging of white matter integrity?

PERTINENT FINDINGS: We prospectively investigated ^{11}C -PiB and ^{18}F -flutemetamol uptake in WMH and NAWM in 61 CU adults. WMH and NAWM SUVrs were higher with ^{18}F -flutemetamol than ^{11}C -PiB in both older and in younger CU adults. ^{11}C -PiB and ^{18}F -flutemetamol SUVrs were higher in older than in younger CU adults in both WMH and in NAWM. ^{11}C -PiB and ^{18}F -flutemetamol showed a similar topographic pattern of uptake, with higher SUVr in NAWM than in WMH in both older and younger CU adults. There was no difference between ^{11}C -PiB versus ^{18}F -flutemetamol SUVrs in differentiating WMH from NAWM in both older and younger CU adults.

IMPLICATIONS FOR PATIENT CARE: With a longer half-life and commercial availability, ^{18}F -flutemetamol may be an appealing alternative to ^{11}C -PiB for molecular imaging in demyelinating diseases such as MS to evaluate myelin integrity in clinical trials targeting myelin repair.

REFERENCES

1. Stankoff B, Wang Y, Bottlaender M, et al. Imaging of CNS myelin by positron-emission tomography. *Proc Natl Acad Sci USA*. 2006;103:9304–9309.
2. Stankoff B, Freeman L, Aigrot MS, et al. Imaging central nervous system myelin by positron emission tomography in multiple sclerosis using [methyl- ^{11}C]-2-(4'-methylaminophenyl)-6-hydroxybenzothiazole. *Ann Neurol*. 2011;69:673–680.
3. Faria DP, Copray S, Sijbesma JW, et al. PET imaging of focal demyelination and remyelination in a rat model of multiple sclerosis: comparison of [^{11}C]MeDAS, [^{11}C]CIC and [^{11}C]PiB. *Eur J Nucl Med Mol Imaging*. 2014;41:995–1003.
4. Matias-Guiu JA, Cabrera-Martin MN, Matias-Guiu J, et al. Amyloid PET imaging in multiple sclerosis: an ^{18}F -florbetaben study. *BMC Neurol*. 2015;15:243.
5. Veronese M, Bodini B, Garcia-Lorenzo D, et al. Quantification of [^{11}C]PiB PET for imaging myelin in the human brain: a test-retest reproducibility study in high-resolution research tomography. *J Cereb Blood Flow Metab*. 2015;35:1771–1782.
6. Bodini B, Veronese M, Garcia-Lorenzo D, et al. Dynamic imaging of individual remyelination profiles in multiple sclerosis. *Ann Neurol*. 2016;79:726–738.
7. Zeydan B, Lowe VJ, Schwarz CG, et al. Pittsburgh compound-B PET white matter imaging and cognitive function in late multiple sclerosis. *Mult Scler*. 2018;24:739–749.
8. Zeydan B, Schwarz CG, Lowe VJ, et al. Investigation of white matter PiB uptake as a marker of white matter integrity. *Ann Clin Transl Neurol*. 2019;6:678–688.
9. Pytel V, Matias-Guiu JA, Matias-Guiu J, et al. Amyloid PET findings in multiple sclerosis are associated with cognitive decline at 18 months. *Mult Scler Relat Disord*. 2020;39:101926.
10. Zhang M, Ni Y, Zhou Q, et al. ^{18}F -florbetapir PET/MRI for quantitatively monitoring myelin loss and recovery in patients with multiple sclerosis: a longitudinal study. *EClinicalMedicine*. 2021;37:100982.
11. Bauckneht M, Capitanio S, Raffia S, et al. Molecular imaging of multiple sclerosis: from the clinical demand to novel radiotracers. *EJNMMI Radiopharm Chem*. 2019;4:6.
12. Bodini B, Tonietto M, Airas L, Stankoff B. Positron emission tomography in multiple sclerosis - straight to the target. *Nat Rev Neurol*. 2021;17:663–675.
13. Lowe VJ, Lundt E, Knopman D, et al. Comparison of [^{18}F]flutemetamol and [^{11}C]Pittsburgh compound-B in cognitively normal young, cognitively normal elderly, and Alzheimer's disease dementia individuals. *Neuroimage Clin*. 2017;16:295–302.
14. Brendel M, Hogenauer M, Delker A, et al. Improved longitudinal [^{18}F]-AV45 amyloid PET by white matter reference and VOI-based partial volume effect correction. *Neuroimage*. 2015;108:450–459.
15. Chen K, Roontiva A, Thiyyagura P, et al. Improved power for characterizing longitudinal amyloid-beta PET changes and evaluating amyloid-modifying treatments with a cerebral white matter reference region. *J Nucl Med*. 2015;56:560–566.
16. Landau SM, Fero A, Baker SL, et al. Measurement of longitudinal beta-amyloid change with ^{18}F -florbetapir PET and standardized uptake value ratios. *J Nucl Med*. 2015;56:567–574.
17. Shokouhi S, McKay JW, Baker SL, et al. Reference tissue normalization in longitudinal ^{18}F -florbetapir positron emission tomography of late mild cognitive impairment. *Alzheimers Res Ther*. 2016;8:2.
18. Schwarz CG, Senjem ML, Gunter JL, et al. Optimizing PiB-PET SUVR change-over-time measurement by a large-scale analysis of longitudinal reliability, plausibility, separability, and correlation with MMSE. *Neuroimage*. 2017;144:113–127.
19. Garnier-Crussard A, Bougacha S, Wirth M, et al. White matter hyperintensities across the adult lifespan: relation to age, Abeta load, and cognition. *Alzheimers Res Ther*. 2020;12:127.
20. Nelissen N, Van Laere K, Thurfjell L, et al. Phase 1 study of the Pittsburgh compound B derivative ^{18}F -flutemetamol in healthy volunteers and patients with probable Alzheimer disease. *J Nucl Med*. 2009;50:1251–1259.
21. Lowe VJ, Kemp BJ, Jack CR, Jr., et al. Comparison of ^{18}F -FDG and PiB PET in cognitive impairment. *J Nucl Med*. 2009;50:878–886.
22. Raz L, Jayachandran M, Tosakulwong N, et al. Thrombogenic microvesicles and white matter hyperintensities in postmenopausal women. *Neurology*. 2013;80:911–918.
23. Schwarz CG, Gunter JL, Ward CP, et al. The Mayo Clinic Adult Life Span Template: better quantification across the life span. *Alzheimers Dement*. 2017;13(suppl):P93–P94.
24. Xu H, Qian J, Paynter NP, et al. Estimating the receiver operating characteristic curve in matched case control studies. *Stat Med*. 2019;38:437–451.
25. Vandenberghe R, Van Laere K, Ivanoiu A, et al. ^{18}F -flutemetamol amyloid imaging in Alzheimer disease and mild cognitive impairment: a phase 2 trial. *Ann Neurol*. 2010;68:319–329.
26. Villemagne VL, Mulligan RS, Pejoska S, et al. Comparison of ^{11}C -PiB and ^{18}F -florbetaben for Abeta imaging in ageing and Alzheimer's disease. *Eur J Nucl Med Mol Imaging*. 2012;39:983–989.
27. Wu C, Wang C, Popescu DC, et al. A novel PET marker for in vivo quantification of myelination. *Bioorg Med Chem*. 2010;18:8592–8599.

28. Wu C, Zhu J, Baeslack J, et al. Longitudinal positron emission tomography imaging for monitoring myelin repair in the spinal cord. *Ann Neurol*. 2013;74:688–698.
29. Hatashita S, Yamasaki H, Suzuki Y, Tanaka K, Wakebe D, Hayakawa H. [¹⁸F]Flutemetamol amyloid-beta PET imaging compared with [¹¹C]PiB across the spectrum of Alzheimer's disease. *Eur J Nucl Med Mol Imaging*. 2014;41:290–300.
30. Mountz JM, Laymon CM, Cohen AD, et al. Comparison of qualitative and quantitative imaging characteristics of [¹¹C]PiB and [¹⁸F]flutemetamol in normal control and Alzheimer's subjects. *Neuroimage Clin*. 2015;9:592–598.
31. Auvity S, Tonietto M, Caille F, et al. Repurposing radiotracers for myelin imaging: a study comparing ¹⁸F-florbetaben, ¹⁸F-florbetapir, ¹⁸F-flutemetamol, ¹¹C-MeDAS, and ¹¹C-PiB. *Eur J Nucl Med Mol Imaging*. 2020;47:490–501.
32. Moscoso A, Silva-Rodriguez J, Aldrey JM, et al. ¹⁸F-florbetapir PET as a marker of myelin integrity across the Alzheimer's disease spectrum. *Eur J Nucl Med Mol Imaging*. 2022;49:1242–1253.
33. Klunk WE, Pettegrew JW, Abraham DJ. Quantitative evaluation of Congo red binding to amyloid-like proteins with a beta-pleated sheet conformation. *J Histochem Cytochem*. 1989;37:1273–1281.
34. Ridsdale RA, Beniac DR, Tompkins TA, Moscarello MA, Harauz G. Three-dimensional structure of myelin basic protein. II. Molecular modeling and considerations of predicted structures in multiple sclerosis. *J Biol Chem*. 1997;272:4269–4275.
35. Klunk WE, Engler H, Nordberg A, et al. Imaging brain amyloid in Alzheimer's disease with Pittsburgh Compound-B. *Ann Neurol*. 2004;55:306–319.
36. Fodero-Tavoletti MT, Rowe CC, McLean CA, et al. Characterization of PiB binding to white matter in Alzheimer disease and other dementias. *J Nucl Med*. 2009;50:198–204.
37. Lowe VJ, Lundt ES, Senjem ML, et al. White matter reference region in PET studies of ¹¹C-Pittsburgh Compound B uptake: effects of age and amyloid-beta deposition. *J Nucl Med*. 2018;59:1583–1589.
38. Ichise M, Golan H, Ballinger JR, Vines D, Blackman A, Moldofsky H. Regional differences in technetium-99m-ECD clearance on brain SPECT in healthy subjects. *J Nucl Med*. 1997;38:1253–1260.
39. van Gelderen P, de Zwart JA, Duyn JH. Pitfalls of MRI measurement of white matter perfusion based on arterial spin labeling. *Magn Reson Med*. 2008;59:788–795.
40. Fisher JP, Hartwich D, Seifert T, et al. Cerebral perfusion, oxygenation and metabolism during exercise in young and elderly individuals. *J Physiol (Lond)*. 2013;591:1859–1870.